RESOLUTION BOUND AND DETECTION RESULTS FOR SCATTERING CENTERS*

William M. Steedly,[1] Ching-Hui J. Ying,[2] and Randolph L. Moses[2]

[1]The Analytic Sciences Corporation, USA
[2]The Ohio State University, USA

INTRODUCTION

This paper is concerned with detection and estimation of the scattering centers of a target from coherent, stepped frequency measurements. In particular, we are interested in the following questions: 1) how closely spaced can scattering centers be before it is impossible to resolve them, and 2) what is the relationship between the detection probability of a scattering center and the false alarm probability as a function of scattering center SNR.

To address these questions, we hypothesize a parametric model of target scattering. This model assumes the frequency-domain scattering to be a sum of exponential terms. If the exponential terms are undamped, then the model specializes to a point-scatterer assumption. If the exponential terms are not undamped, the model incorporates frequency-dependent radar cross section of scattering centers (see (1)). We consider a particular class of algorithms for estimating the parameters in this exponential model, the so-called total-least squares (TLS) Prony algorithm (2). The TLS-Prony technique has gained popularity as a parameter estimation algorithm for the exponential model because it provides accurate parameter estimates at moderate computational cost (3); it has also been successfully applied to both one-dimensional and two-dimensiaonal radar scattering data (4,5).

Under the exponential model assumption of scattering, the resolution and detection bounds can be reformulated in terms of parameter estimation accuracy for the exponential model. We present the asymptotic (as SNR $\rightarrow \infty$) probability density function (pdf) for the exponential model parameter estimates using the TLS-Prony algorithm. We then use this asymptotic pdf to derive scattering center resolution and detection bounds for the TLS-Prony algorithm, and compare these results to Cramér-Rao bound (CRB) results. Monte-Carlo simulations are also presented to compare with the theory. The resolution bounds are obtained from the standard deviation bounds of the pole angles in the exponential models. The detection bounds are obtained by considering the probability that the energy of an estimated mode exceeds a pre-defined threshold. In each case, the probabilities are obtained by considering a high-SNR approximation of the statistical probabilities of exponential model parameter estimates.

One of the advantages of a model-based scattering center estimation procedure is the capability of resolving scattering centers more accurately than is possible using fast Fourier Transform (FFT) techniques. We show that for sufficiently high SNR, both the CRB resolution and the TLS-Prony resolution is better than can be obtained using the FFT.

*THIS RESEARCH WAS SUPPORTED IN PART BY THE AIR FORCE OFFICE OF SCIENTIFIC RESEARCH, THE AVIONICS DIVISION, WRIGHT LABORATORIES, AND THE SURVEILLANCE DIVISION, ROME LABORATORIES.

DATA MODEL AND TLS-PRONY ESTIMATION PROCEDURE

Data Model

Assume the data vector y of length m is modeled as a noisy exponential sequence

$$y_q = \sum_{i=1}^{n} x_i p_i^q + e_q \qquad q = 0, 1, \ldots, m-1. \tag{1}$$

There are n distinct exponential modes in the data. Here, it is assumed that $\{e_q\}$ is a zero mean complex white Gaussian noise sequence with variance σ. Equation 1 may be compactly written as

$$y = Ax + e, \tag{2}$$

where e $(m \times 1)$ and x $(n \times 1)$ are vectors, and

$$A = \begin{bmatrix} 1 & 1 & \cdots & 1 \\ p_1 & p_2 & \cdots & p_n \\ \vdots & \vdots & & \vdots \\ p_1^{m-1} & p_2^{m-1} & \cdots & p_n^{m-1} \end{bmatrix}. \tag{3}$$

TLS-Prony Estimation Procedure

In this subsection we give an overview of the TLS-Prony technique (2) which is used to estimate the parameters of the exponential model presented in Equation 2.

First, Lth order backward linear prediction equations are formed:

$$\begin{bmatrix} y & Y \end{bmatrix} \begin{bmatrix} 1 \\ b \end{bmatrix} \approx 0, \tag{4}$$

where

$$b = \begin{bmatrix} b_1 & b_2 & \cdots & b_L \end{bmatrix}^T \tag{5}$$

and where

$$\begin{bmatrix} y & Y \end{bmatrix} = \begin{bmatrix} y_0 & y_1 & \cdots & y_L \\ y_1 & y_2 & \cdots & y_{L+1} \\ \vdots & \vdots & & \vdots \\ y_{m-(L+1)} & y_{m-L} & \cdots & y_{m-1} \end{bmatrix}. \tag{6}$$

In general, $L \geq n$; however, choosing $L > n$ results in more accurate parameter estimates (6).

The solution of Equation 4 involves obtaining an SVD of the matrix $\begin{bmatrix} y & Y \end{bmatrix}$ and truncating all but the first n singular values to arrive at an estimate $\begin{bmatrix} \hat{y} & \hat{Y} \end{bmatrix}$. The linear prediction coefficient vector estimate $\hat{b}$ is found as $\hat{b} = -\hat{Y}^{+}\hat{y}$, where $^{+}$ denotes the Moore-Penrose pseudoinverse. Finally, the pole estimates are found by

$$\hat{p}_j = \text{zero}_j\left(\hat{B}(z)\right), \qquad j = 1, 2, \ldots, L. \tag{7}$$

where $\hat{B}(z) = 1 + \hat{b}_1 z + \cdots + \hat{b}_L z^L$. Once the poles have been determined, the amplitude coefficients can be found

as the least squares solution to

$$\begin{bmatrix} 1 & 1 & \cdots & 1 \\ \widehat{p}_1 & \widehat{p}_2 & \cdots & \widehat{p}_L \\ \widehat{p}_1^2 & \widehat{p}_2^2 & \cdots & \widehat{p}_L^2 \\ \vdots & \vdots & & \vdots \\ \widehat{p}_1^{m-1} & \widehat{p}_2^{m-1} & \cdots & \widehat{p}_L^{m-1} \end{bmatrix} \begin{bmatrix} \widehat{x}_1 \\ \widehat{x}_2 \\ \vdots \\ \widehat{x}_L \end{bmatrix} \approx \mathrm{y}. \quad (8)$$

Note that L mode estimates are obtained, of which n are "true" modes. For $L > n$, $L - n$ of the mode estimates are extraneous. If n is known then the true modes can be identified as the n highest energy estimates (3). However, in practice n is typically unknown; in this case the number of singular values retained is a fixed upper bound of n, and true modes could be separated from extraneous modes by using a mode energy threshold (as discussed below).

STATISTICAL ANALYSIS

In order to establish a resolution bound and probabilities of detection and false alarm, we need the statistics for the estimated parameters in the TLS-Prony model. For the resolution bounds and detection probabilities, we need only the statistics for the "true" modes (that is, the n modes with highest energies). For this case, the statistics of the parameter estimates have been found in (3,7). However, for the false alarm probability, we also need the statistics of the $L-n$ extraneous modes. The derivation of the extraneous mode statistics appears in (8); the main result is summarised in the following Theorem.

Theorem 1: Assume y is as given in Equation 1. Let $p = \{p_i\}_{i=1}^n$ and $x = \{x_i\}_{i=1}^n$ be as in Equation 1, and let $p^e = \{p_i^e\}_{i=1}^{L-n}$ and $x^e = \{x_i^e\}_{i=1}^{L-n}$ denote the $L-n$ extraneous modes obtained in the TLS-Prony procedure when $\sigma = 0$. Let θ denote the $4L \times 1$ vector containing the angles and magnitudes of p, x, p^e, and x^e, respectively, and let $\widehat{\theta}$ denote the TLS-Prony estimate of θ. Then the asymptotic (as $\sigma \to 0$) probability density function of $\widehat{\theta}$ is Gaussian:

$$\widehat{\theta} \sim N(\theta, \sigma \cdot \Sigma_\theta), \quad (9)$$

where Σ_θ is a covariance matrix which depends on m, L, and $\{x_i, p_i\}_{i=1}^L$.

The proof of the Theorem and an explicit expression for Σ_θ, can be found in (8). Also in (8) is an expression for Σ_θ when θ is reparameterized in terms of the real and imaginary parts of the poles and amplitude coefficients. We note that the above Theorem gives a theoretical expression for the complete pdf of the estimated parameters; this pdf can then be used to study the resolution properties and detection probabilities of scattering centers, as is discussed below.

A RESOLUTION CRITERION AND BOUND ANALYSIS

Consider two poles on the unit circle, $p_1 = \alpha_1 e^{j\omega_1}$ and $p_2 = \alpha_2 e^{j\omega_2}$. We define the resolution limit r as

$$r = 2\sigma_{\omega_1} + 2\sigma_{\omega_2}, \quad (10)$$

where the angle variances of p_1 and p_2 are $\sigma_{\omega_1}^2$ and $\sigma_{\omega_2}^2$, respectively. When two poles are at this limit, the 95% confidence intervals of the angle estimates for each pole become disjoint.

The CRB resolution limit is found by using CRB expressions for the pole angles in two pole model. The CRBs for the pole angles are inserted into σ_{ω_1} and σ_{ω_2} in Equation 10; such expressions can be found, for example, in (9). This limit gives a lower bound for all unbiased estimators since it is based on the CRB. The resolution limit for the TLS-Prony estimation algorithm is similarly given by using pole angle variance statistics for the true poles; these are readily obtained from $\sigma \cdot \Sigma_\theta$ (see (8)).

Bound Analysis for Two Undamped Modes

In this study we consider two equal energy modes located on the unit circle at $p_1 = e^{j\pi f/m}$ and $p_2 = e^{-j\pi f/m}$ for a data length of $m = 10$, where f is the separation of the two modes in Fourier bins. For the TLS-Prony simulations a prediction order of $L = 4$ was used.

Figure 1 shows the bounds for the CRB, TLS-Prony statistical theory, and TLS-Prony Monte-Carlo results. The axes are normalized to make the curves independent of data length for the CRB curve and the TLS-Prony statistical theory curve. From these curves we can see that the TLS-Prony theoretical bound is quite close to the CRB over a wide range of SNR. Recall that the CRB and TLS-Prony bounds are both derived using small perturbation analysis, so hold only for high SNR. The TLS-Prony Monte Carlo simulations show good agreement with the theoretical bound above 15 dB SNR. We can see that above 20dB SNR/pole/bin the TLS-Prony method virtually achieves the CRB.

Below 20dB SNR/pole/bin, the Monte-Carlo simulations give much higher variance than both the theoretical TLS-Prony curve and the CRB curve. Note, however, that the TLS-Prony analytical variance expression was derived under the assumption of high SNR, and is not expected to be accurate at low SNR. In addition, the CRB is not necessarily a tight bound at low SNR. Thus, it is not clear what the minimum achievable variance is in this region. For example, it is not known whether (or how much) an iterative maximum likelihood procedure would result in lower variance in this region.

We note that above about 18 dB SNR/pole/bin, the TLS-Prony technique gives resolutions of less than one Fourier bin. Therefore, the resolution of the TLS-Prony technique is better than FFT-based techniques since FFT-based techniques can only resolve to within one Fourier bin. If windowing is used in conjunction with the FFT-based methods, their resolution is even larger than one Fourier bin (*e.g.*, it would be about 1.8 Fourier bins using a Hamming window).

DERIVATION OF PROBABILITIES OF DETECTION AND FALSE ALARM

In practice, one does not know *a priori* how many scattering centers are present. In this case, one would accept or reject a mode estimate as a scattering center based on some threshold. We consider a threshold on the energy of the estimated exponential mode, as this corresponds to radar cross section of an estimated scattering center.

In the TLS-Prony method, one obtains estimates of L poles and L corresponding amplitude coefficients. From this, one can compute the energy E_j of each of the L modes by

$$E_j = \beta_j^2 \sum_{q=0}^{m-1} \alpha_j^{2q}, \quad j = 1, 2, \ldots, L, \quad (11)$$

where β_j and α_j are the magnitudes of the jth amplitude coefficient and pole, respectively. We consider an estimated mode to be detected as a valid scattering center if its energy exceeds a prespecified threshold, and we

reject the mode as an invalid scattering center if it does not. We then can present detection results in the form of receiver operation characteristic (ROC) curves.

Probability of Detection

We define a detection to be the case in which all of the true mode energy estimates exceed an energy threshold, E^0. We thus now derive the energy statistics for the true modes (*i.e.*, $j = 1, 2, \ldots, n$). These statistics can be found from the statistical pdf given in Theorem 1. It can be shown (8) that the energies are noncentral χ^2 distributed; for high SNR, the noncentral χ^2 distribution is well-approximated by a Gaussian distribution. Using first-order approximations, it is possible to derive the mean and covariance of this distribution. Thus, from Theorem 1 we have the following corollary.

Corollary 1: Let

$$E = [\ E_1 \quad E_2 \quad \cdots \quad E_n\ ]^T, \tag{12}$$

denote the parameter vector for the mode energies of the true modes (*i.e.*, the mode energies corresponding to p and x). Let $\widehat{E}$ denote the estimated energies corresponding to the TLS-Prony parameter estimates. Then the asymptotic (as $\sigma \to 0$) pdf of E is given by

$$\widehat{E} \sim N(E, \sigma \cdot \Sigma_E), \tag{13}$$

where Σ_E depends on m, L, and $\{x_i, p_i\}_{i=1}^n$. An explicit expression for Σ_E can be found in (8).

Given the true mode energy distribution, the probabilty of detection, P_D, is given by

$$P_D = \Pr\left(\widehat{E_1} > E^0, \widehat{E_2} > E^0, \ldots, \widehat{E_n} > E^0\right). \tag{14}$$

This probability is readily computed using Equation 13.

To verify that the theoretical energy distribution given above, Monte-Carlo simulations were performed for a two mode case. In this case, the data consists of two equal energy modes, with $x_1 = x_2 = 1$, located on the unit circle spaced one Fourier bin apart at $p_1 = e^{j2\pi/m}$ and $p_2 = e^{-j2\pi/m}$ for a data length of $m = 10$. A prediction order of $L = 4$ was used, and two singular values were retained. The SNR for these simulations was 10dB/pole.

Figure 2 shows a comparison between the theoretical pdf and a histogram obtained from Monte-Carlo simulations (note that both modes have the same theoretical pdfs and had similar histograms). It can be seen that the theoretical energy distribution is a good approximation to simulation results in this case.

Probability of False Alarm

We define a false alarm to be the case in which one or more of the extraneous modes is above the energy threshold, E^0, and thus misidentified as a true mode. We can derive the statistal properties of the estimated extraneous mode energies in a similar manner as above. In this case, however, the "true" energies of the extraneous modes are zero, so the extraneous modes are distributed as central Chi-squared with two degrees of freedom, χ_2^2 (see (8)). This is stated in the following corollary.

Corollary 2: Let $\left\{\widehat{E_i^e}\right\}_{i=1}^{L-n}$ denote the estimated energies corresponding to the TLS-Prony parameter estimates of the extraneous mode energies. Then the asymptotic (as $\sigma \to 0$) pdfs of these energies are given by

$$\widehat{E_i^e} \sim \chi_2^2\left(\sigma \cdot \Sigma_{E_i^e}\right) \qquad i = 1, 2, \ldots, L-n. \tag{15}$$

where $\Sigma_{E_i^e}$ does not depend on σ. An explicit expression for $\Sigma_{E_i^e}$ can be found in (8).

Given the extraneous mode energy distributions, the probabilty of false alarm, P_{FA}, is given by

$$P_{FA} = 1 - \Pr\left(\widehat{E_1^e} < E^0, \widehat{E_2^e} < E^0, \ldots, \widehat{E_{L-n}^e} < E^0\right). \tag{16}$$

Note that since the extraneous mode energy distribution is Chi-squared with two degrees of freedom, P_{FA} can be evaluated using a Rayleigh distribution.

Figure 3 shows a comparison between the theoretical pdf for the extraneous modes in the previous two modes example and a histogram obtained from Monte-Carlo simulations. Note that the theoretical predictions agree closely with Monte-Carlo simulations.

ROC Analysis for Two Undamped Modes

Using the above detection and false alarm probability results, we can derive ROC curves for scattering center detection at various SNRs. Figure 4 presents such curves for the case considered in Figures 2 and 3, but with varying SNR (note that $1 - P_D$ is actually plotted along the vertical axis). For an SNR at or above 10dB per pole, P_D is always above 0.9 even when P_{FA} is very small (*e.g.*, 10^{-7}). However this is not the case for lower SNR. Note that for low SNRs P_D never reaches one even if P_{FA} is one. This is because the true mode energy distributions were approximated as Gaussian, and the tail of this Gaussian distribution gives a nonzero probability of a negative energy (the noncentral χ_2^2 distribution does not have such a tail). For high SNR, the approximation becomes more valid.

In computing the curves in Figure 4, it was assumed that the extraneous mode energy distributions are independent. Note that this is a worst case assumption, since P_{FA} would decrease if the extraneous mode energies were dependent.

CONCLUSIONS

In the paper we presented resolution bounds and detection results for estimating the scattering centers. These bounds are based on an exponential model of target scattering, which generalizes the point scattering model. The popular TLS-Prony algorithm was used to estimate the parameters of the exponential model. A high SNR statistical analysis of the TLS-Prony algorithm was first presented. Then, based on the results of the statistical analysis, both resolution bounds and detection results were presented. The resolution bounds were compared with both the Cramér-Rao Bound and with Monte-Carlo simulations. It was shown that for an SNR above 18 dB, the TLS-Prony method is capable of resolution to less than a Fourier bin.

The probabilities of the detection and the the false alarm were derived based on the mode energy distributions for both the true and the extraneous modes. For high SNR true mode energy distributions can be approximated as Gaussian distributions, but extraneous mode energy distributions are central chi-squared distributed. These detection and false alarm probabilities can be presented as ROC curves for scattering center detection for examples of interest.

REFERENCES

1. M. P. Hurst and R. Mittra, "Scattering center analysis via Prony's method," *IEEE Trans. Antennas and Propagation*, vol. AP-35, pp. 986–988, Aug. 1987.

2. M. A. Rahman and K.-B. Yu, "Total least squares approach for frequency estimation using linear prediction," *IEEE Trans. on Acoustics, Speech, and Signal Processing*, vol. ASSP–35, pp. 1440–1454, Oct. 1987.

3. W. M. Steedly, C. J. Ying, and R. L. Moses, "Statistical analysis of TLS-based Prony techniques," *Automatica*, Submitted for publication.

4. W. M. Steedly and R. L. Moses, "High resolution exponential modeling of fully polarized radar returns," *IEEE Trans. on Aerospace and Electronic Systems*. (to appear).

5. J. J. Sacchini, W. M. Steedly, and R. L. Moses, "Two-dimensional prony modeling and parameter estimation," *IEEE Trans. on Signal Processing*, Submitted for publication.

6. P. Stoica, T. Söderström, and F. Ti, "Asymptotic properties of the high-order Yule-Walker estimates of sinusoidal frequencies," *IEEE Trans. on Acoustics, Speech, and Signal Processing*, vol. ASSP–37, pp. 1721–1734, Nov. 1989.

7. W. M. Steedly, C. J. Ying, and R. L. Moses, "Statistical analysis of SVD-Based prony techniques," in *Proceedings of the Twenty-Fifth Asilomar Conference on Signals, Systems, and Computers*, (Pacific Grove, CA), pp. 232–236, November 4–6 1991.

8. C. J. Ying, W. M. Steedly, and R. L. Moses, "Statistical analysis of true and extraneous tls-prony mode estimates," tech. rep., The Ohio State University, Department of Electrical Engineering, ElectroScience Laboratory, 1992.

9. W. M. Steedly and R. L. Moses, "The Cramér-Rao bound for pole and amplitude estimates of damped exponential signals in noise," in *Proceedings of the International Conference on Acoustics, Speech, and Signal Processing*, (Toronto, Ontario), pp. 3569–3572, May 14–17, 1991.

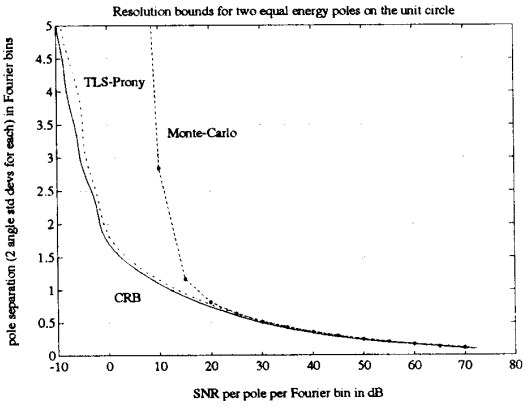

Figure 1: Resolution bounds for two equal energy undamped modes.

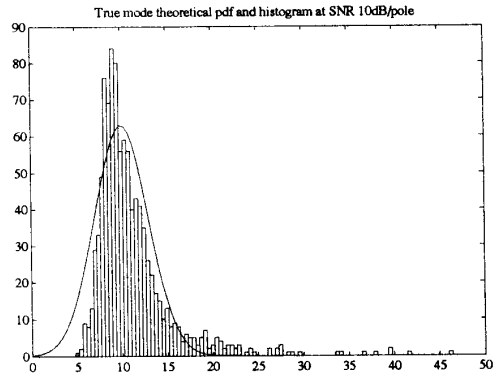

Figure 2: True mode theoretical pdf and histogram for two equal energy undamped modes.

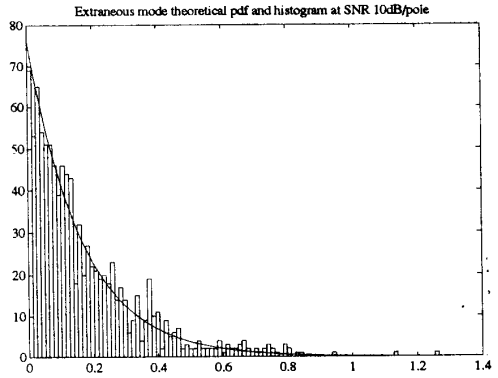

Figure 3: Extraneous mode theoretical pdf and histogram for two equal energy undamped modes.

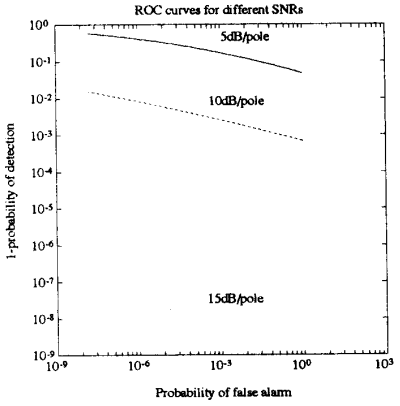

Figure 4: ROC curves for two equal energy undamped modes.